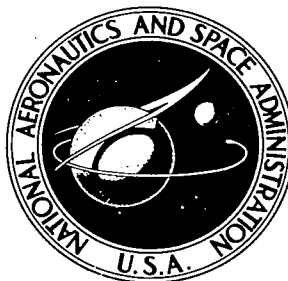


**NASA TECHNICAL NOTE**



**NASA TN D-6193**

*2.1*

**NASA TN D-6193**

**LOAN COPY: R  
AFWL (DC)  
KIRTLAND AI**

**DL33276**



**TECH LIBRARY KAFB, NM**

**TO**

**DYNAMIC AND STATIC WIND-TUNNEL TESTS  
OF A FLOW-DIRECTION VANE**

*by Norman R. Richardson*

*Langley Research Center*

*Hampton, Va. 23365*



**ERRATA**

**NASA Technical Note D-6193**

**DYNAMIC AND STATIC WIND-TUNNEL TESTS  
OF A FLOW-DIRECTION VANE**

**By Norman R. Richardson**

**April 1971**

**Pages 18 and 19:** The time histories shown in figure 9(a) are for test condition 2 and those shown in figure 9(b) are for test condition 1. Therefore, the two figures should be interchanged.

NASA-Langley, 1971

**Issued October 1971**



0133276

1. Report No. NASA TN D-6193		2. Government Accession No.		3. Recipient's Catalog No.	
4. Title and Subtitle DYNAMIC AND STATIC WIND-TUNNEL TESTS OF A FLOW-DIRECTION VANE				5. Report Date April 1971	
				6. Performing Organization Code	
7. Author(s) Norman R. Richardson				8. Performing Organization Report No. L-7431	
9. Performing Organization Name and Address NASA Langley Research Center Hampton, Va. 23365				10. Work Unit No. 720-04-10-01	
				11. Contract or Grant No.	
12. Sponsoring Agency Name and Address National Aeronautics and Space Administration Washington, D.C. 20546				13. Type of Report and Period Covered Technical Note	
				14. Sponsoring Agency Code	
15. Supplementary Notes					
16. Abstract  Dynamic and static wind-tunnel tests of a low-inertia flow-direction vane are described in this report. This vane was designed by NASA to provide good dynamic response characteristics and has been used for the in-flight measurement of gust velocities. Both subsonic and supersonic tests were conducted. The data indicated that the natural frequency of the vane is about one-half times the square root of the dynamic pressure (measured in $N/m^2$ ) or about three times the square root of the dynamic pressure (measured in psf). The data also indicated that the damping ratio is between 0.80 and 0.65 critical at sea level and varies approximately as the square root of the air density.					
17. Key Words (Suggested by Author(s))  Flow-direction vane Dynamic test			18. Distribution Statement  Unclassified - Unlimited		
19. Security Classif. (of this report) Unclassified		20. Security Classif. (of this page) Unclassified		21. No. of Pages 21	
				22. Price* \$3.00	

# DYNAMIC AND STATIC WIND-TUNNEL TESTS OF A FLOW-DIRECTION VANE

By Norman R. Richardson  
Langley Research Center

## SUMMARY

Dynamic and static wind-tunnel tests of a low-inertia flow-direction vane are described in this report. This vane was designed by NASA to provide good dynamic response characteristics and has been used for the in-flight measurement of gust velocities. Both subsonic and supersonic tests were conducted. The data indicated that the natural frequency of the vane is about one-half times the square root of the dynamic pressure (measured in  $\text{N/m}^2$ ) or about three times the square root of the dynamic pressure (measured in psf). The data also indicated that the damping ratio is between 0.80 and 0.65 critical at sea level and varies approximately as the square root of the air density.

## INTRODUCTION

An important use of flow-direction devices in flight tests is in the measurement of gust velocities. If the device has a good dynamic response to incremental flow-direction changes, it will provide a measurement of the resultant of the airplane air-speed and a gust velocity normal to the measuring axis. The data from the flow-direction measurement, in conjunction with measurements of airplane motion, permit the extraction of gust velocity (ref. 1). Differential pressure probes, fixed airfoils on load balances, and weathercock-type free-trailing vanes have all been used for such measurements; each has some disadvantages, either mechanically or in the indirect nature of the measurement. For several years, NASA has favored the use of the free-trailing vane because it provides a direct measurement of flow angle as a null-seeking device; hence, a precise knowledge of its aerodynamic coefficients is not needed in data interpretation. The vanes used for gust measurements are constructed primarily of balsa wood to provide the low inertia required for a high natural frequency and good aerodynamic damping. This basic design has been in use for several years and some undocumented wind-tunnel tests were conducted at low-speed and sea-level density to determine that the dynamic performance was adequate for the intended use. Since that time, the conditions under which the vane has been used have expanded considerably both in air-speed and altitude.

The purpose of this investigation was to extend the range of test conditions and to obtain a more detailed knowledge of the vane performance. The natural frequency and damping ratio of the vane as related to airspeed and air density are the parameters of primary concern. Time-history records were made of the vane response to step-function inputs to provide data on these parameters. In addition, wind-tunnel tests were conducted to measure the vane hinge moment as a function of angle of attack; these data were used for the derivation of the undamped natural frequency of the vane and the interpretation of the dynamic-response data.

Tests at Mach numbers of 0.183 and 0.268 were conducted in the Langley low-turbulence pressure tunnel. Tests at a Mach number of 1.6 were conducted in the Langley 4- by 4-foot supersonic pressure tunnel. Data on the measured dynamic response and static moment will be presented in this paper. Some of the high-dynamic-pressure flight conditions under which the vane has been used will also be presented.

## SYMBOLS

Measurements and calculations were made in the U.S. Customary Units; however, they are presented in both the International System of Units (SI) and the U.S. Customary Units herein.

$d$	center-of-pressure distance from hinge axis, m (in.)
$f_n$	undamped natural frequency, Hz
$I$	moment of inertia, $\text{kg-m}^2$ (in-lbf-sec <sup>2</sup> )
$K$	measured hinge-moment slope, $\text{m-N/rad}$ (in-lbf/rad)
$K_O$	hinge-moment constant, $K/q, \frac{\text{m-N}}{\text{N/m}^2} \left( \frac{\text{in-lbf}}{\text{psf}} \right)$
$K'$	measured hinge-moment slope about offset axis, $\text{m-N/rad}$ (in-lbf/rad)
$L$	lift force, N (lbf)
$M$	Mach number
$p_O$	static pressure, $\text{N/m}^2$ (psf)
$q$	dynamic pressure, $\text{N/m}^2$ (psf)

T	total temperature, °K
x	offset distance, m (in.)

## APPARATUS AND TESTS

### Vanes

The vane is a rectangular, flat-plate configuration with an aspect ratio of 0.5 and is constructed of laminated balsa wood. The vane is bonded to a stainless-steel leading edge and shaft adapter as shown in figure 1. An extension from the leading edge, located inboard of the vane, provides the mass balance for the assembly.

Two different vanes are shown in figure 1; one is tapered at the trailing edge to one-half the thickness of the leading edge and the other has a constant thickness. The tapered version has been used for subsonic flight tests and was used for the subsonic tests in this investigation; the untapered version has been used for supersonic flight tests and was used for the supersonic tests in this investigation.

The moment of inertia of the average subsonic vane is  $0.158 \times 10^{-4} \text{ kg-m}^2$  ( $1.4 \times 10^{-4} \text{ in-lbf-sec}^2$ ) and that of the average supersonic vane is  $0.241 \times 10^{-4} \text{ kg-m}^2$  ( $2.13 \times 10^{-4} \text{ in-lbf-sec}^2$ ). The moment of inertia of the shaft and position transmitter is about 2 percent of that of the vane.

### Vane Mounting

The vanes normally are used in pairs installed either on a combined pitot-static tube, flow-direction transducer as shown in figure 2 or on a pod type of housing as shown in figure 3. This pod type of housing has been used only for subsonic flight tests. The vane assembly is pinned to a steel shaft which is free to rotate in a hollow strut that projects from the housing. The outboard end of the shaft fits in a bronze sleeve bearing; the inboard end of the shaft normally is attached to the shaft of either a synchro or a low-torque potentiometer, depending on the system application. A nose-boom mounting is normally used to place the vanes as far ahead of the airplane as possible, with one vane oriented to respond to changes in angle of attack and the other oriented to respond to changes in angle of sideslip. The single vane tested will be referred to in the angle-of-attack sense.

The pod type of housing was used for the subsonic tests for convenience in making the necessary internal modifications and is shown in figure 4. The test unit was modified for the supersonic tests, as shown in figure 5, by the addition of a simulated pitot-static tube so the vane would be behind the bow shock as it would be in flight at the test Mach number.

### Force-Test Apparatus

For the force tests, the unit was arranged to permit measuring the hinge moment of the vane as a function of the angle of attack and dynamic pressure. The inboard end of the vane shaft was supported in a ball bearing, and a sensitive strain-gage beam was clamped to the shaft extension, as shown in figure 6, to measure the moment on the shaft. An oscillograph was used to record the moment data. The combined flexibility of the balsa vane and strain-gage beam resulted in a vane deflection of about  $13^{\circ}$  per m-N of moment ( $1.5^{\circ}$  per in-lbf of moment); this amount was applied as a correction factor to the test data.

During the subsonic testing, moment data were also taken with the vane mounted on the offset shaft shown in figure 6. This shaft moved the reference axis of the vane a known amount from the moment-measuring axis of the test apparatus. On the basis that the lift force on the vane would only be a function of flow angle, the on-axis and the off-axis measurements of the moment would allow the derivation of the lift force and center-of-pressure components of the pitching moment.

### Dynamic-Test Apparatus

For the dynamic tests, the unit was arranged to permit releasing the vane from initial angles of attack while time-history recordings were made of the vane response. The release mechanism and angular position transmitter installations are shown in figure 7. The inboard end of the vane shaft was attached to the shaft of a small micro-torque potentiometer in the same general arrangement used in flight. The potentiometer, which was of the deposited-film type, was connected into a modified bridge circuit and the output signal was recorded on a direct-write oscillograph using a 100-Hz galvanometer. The release mechanism consisted of a small stop pin inserted through the vane shaft and arranged to bear against the plunger of a solenoid. It was set to restrain the vane at a zero angle with respect to the housing axis.

### Wind-Tunnel Installation and Tests

For each set of tests, the test unit was mounted on the existing sting mechanism in the wind tunnel. These mechanisms allowed setting the test unit at the desired angle of attack while keeping the vane in essentially the same location in the center of the wind-tunnel test section. For the dynamic tests, the sting was first brought to an angle which placed the vane-shaft stop pin on the proper side of the release plunger; the sting was then set at the desired release angle with the vane restrained. A high-speed oscillograph record of the vane angle was taken as the vane was released by the solenoid and assumed the free-trailing position. For the force tests, the vane was set at several

flow angles by the sting mechanism, and oscillograph recordings of the hinge moment were made for each angle.

An angle-of-attack range of only a few degrees was considered necessary in these tests since this is the range of principal concern in the flight-test measurement of gust velocities. In addition, low-aspect-ratio airfoil data (refs. 2, 3, and 4) indicated that the moment gradient for the vane would increase considerably with increasing angle and, therefore, that large angle inputs might not properly indicate the vane performance under its normal usage.

The wind-tunnel conditions (designated 1, 2, and 3) for the principal tests are listed in the following table:

Test condition	Facility	Mach number	q		P <sub>o</sub>		T, °K	Air-density ratio
			N/m <sup>2</sup>	psf	kN/m <sup>2</sup>	psf		
1	Langley low-turbulence pressure tunnel	0.183	2394	50	101.7	2125	300	1.00
2	Langley low-turbulence pressure tunnel	0.268	2394	50	47.7	997	300	0.47
3	Langley 4- by 4-foot supersonic pressure tunnel	1.6	9097	190	5.1	106	310	0.073

The air density for test condition 1 was essentially the same as the standard sea-level density. The densities for the other two test conditions are given in the table as the ratios to condition 1. The wind-tunnel precision manometers and sting-angle readout systems were used for measuring the pressure conditions and the angle of attack.

## RESULTS AND DISCUSSION

### Force Tests

Vane hinge moments were measured under test conditions 1 and 3 ( $M = 0.183$  and  $M = 1.6$ , respectively) and are shown in figure 8. These data, as plotted, have been corrected for the vane deflection under load as mentioned previously. For the subsonic tests, the moment curve is essentially linear over an angle-of-attack range from  $-2^\circ$  to  $2^\circ$ ; above  $2^\circ$ , the slope increases and is about doubled at an angle of attack of  $5^\circ$ . The slope near zero angle of attack will be used for the moment constant in deriving the natural frequency of the vane. This slope  $K$  is  $0.298 \text{ m-N/rad}$  ( $2.64 \text{ in-lbf/rad}$ ) at a dynamic pressure of  $2394 \text{ N/m}^2$  ( $50 \text{ psf}$ ). The moment constant  $K_o$  is then  $1.25 \times 10^{-4} \frac{\text{m-N}}{\text{N/m}^2}$  ( $0.0528 \frac{\text{in-lbf}}{\text{psf}}$ ). For the supersonic tests at Mach 1.6, the



hinge-moment curve is about linear near zero angle with an increasing slope at a somewhat smaller angle of attack than in the subsonic tests. Near zero angle of attack, the slope  $K$  is 1.49 m-N/rad (1.32 in-lbf/rad) at a dynamic pressure of 9097 N/m<sup>2</sup> (190 psf). The moment constant  $K_0$  is then  $1.64 \times 10^{-4} \frac{\text{m-N}}{\text{N/m}^2} \left( 0.0695 \frac{\text{in-lbf}}{\text{psf}} \right)$ .

Additional measurements were made under the subsonic conditions with the vane mounted on the offset shaft previously described; the offset distance  $x$  was 19 mm (0.75 inch). The slope of the moment curve was 0.816 m-N/rad (7.22 in-lbf/rad) compared with 0.298 m-N/rad (2.64 in-lbf/rad) in the normal mounting. Equations for the two measured moments,  $K = Ld$  and  $K' = L(d + x)$ , where  $L$  is the lift force, combine to give the following relation:

$$d = \frac{Kx}{K' - K}$$

Solving for the numerical value of  $d$  and converting to percent chord with respect to the leading edge of the vane indicates a center-of-pressure location for this configuration of 11.3 percent chord at small angles of attack. (The vane pivot axis is at 2.5 percent chord.) The lift force then derived and converted to coefficient form indicates a lift-curve slope of 1.52 per radian.

### Dynamic Tests

Reproductions of the time-history oscillograph records for step-function vane releases under the three test conditions are shown in figure 9. Initial angles of attack for the vane releases range from about 1° to 4°. The vertical grid lines on the records represent a 0.01-second interval. On each part of figure 9, the trace deflection for 1° of vane motion is noted and the deflection is upward at vane release.

The data indicate some variation of the damping ratio, particularly as the region of nonlinear moment is reached; also, the effect of air density is apparent with the damping ratio decreasing as the density is reduced. The damping ratio appears to vary from nearly critical to about 0.25 critical over the range of test conditions. In the supersonic tests (fig. 9(c)), there is some oscillation (or noise) apparent on the records; it has a half-amplitude of about 0.05° at a frequency of about 110 Hz. The source of this noise has not been isolated; possible sources considered were wind-tunnel sting frequency, wind-tunnel flow, electrical or galvanometer pickup, and an inherent vane oscillation. The noise source did appear to be of a transient nature; the amplitude seen on the short section of record in figure 9(c) diminished considerably or disappeared within less than 0.25 second after the release point.

For further interpretation of these response data, the undamped natural frequency of the vane was derived from the relation

$$f_n = \frac{1}{2\pi} \sqrt{\frac{K}{I}} \quad (1)$$

The parameters  $K$ ,  $I$ , and  $f_n$  for the three test conditions are given in the following table:

Test condition	K		I		$f_n$ , Hz	Period, sec	Range of damping ratio	Square root of air-density ratio
	m-N/rad	in-lbf/rad	kg-m <sup>2</sup>	in-lbf-sec <sup>2</sup>				
1	0.298	2.64	$0.158 \times 10^{-4}$	$1.4 \times 10^{-4}$	22	0.045	0.80 to 0.65	1.00
2	0.298	2.64	$0.158 \times 10^{-4}$	$1.4 \times 10^{-4}$	22	0.045	0.65 to 0.50	0.68
3	1.49	13.2	$0.241 \times 10^{-4}$	$2.13 \times 10^{-4}$	40	0.025	0.50 to 0.25	0.27

Based on the derived period, iterative fits were made of theoretical response curves to several of the experimental data. These checks indicated that the vane response was reasonably close to that of a single-degree-of-freedom, second-order system. The range of damping ratios thus obtained for the angle-of-attack ranges covered in figure 9 is shown in the table. For the three test conditions, the damping ratio can be seen to vary approximately as the square root of the air-density ratio. Some theoretical calculations have predicted this relationship.

A few points were taken with the same static pressure as test condition 1 but with the dynamic pressure increased by a factor of three. There was no noticeable change in the damping ratio from that obtained under condition 1.

In equation (1), the natural frequency of the vane is seen to be proportional to the square root of the hinge-moment slope  $K$ . To the extent that the slope  $K$  is linearly related to the dynamic pressure  $q$ , it follows that the natural frequency of the vane is also proportional to the square root of  $q$ . A convenient working relationship of vane frequency to indicated airspeed can also be derived since, for incompressible flow, indicated airspeed is also proportional to the square root of  $q$ . For the subsonic test condition, the vane then had a natural frequency of  $0.45\sqrt{q}$  (for  $q$  measured in N/m<sup>2</sup>) or  $3.1\sqrt{q}$  (for  $q$  measured in psf). For incompressible flow, this corresponds to a frequency of about 0.18 Hz per knot indicated airspeed. At the supersonic test condition, the vane had a natural frequency of  $0.42\sqrt{q}$  (for  $q$  measured in N/m<sup>2</sup>) or  $2.9\sqrt{q}$  (for  $q$  measured in psf).

## Related Tests

In conjunction with the wind-tunnel tests, related tests were conducted to assess the effects of friction on the dynamic response and to confirm experimentally the moment of inertia of the vane. Small springs were attached to the counterweight arm on the vane and adjusted to provide the same moment constant as measured during the wind-tunnel tests (condition 1). The vane was then released from offset angles as it was during the wind-tunnel tests. Observations confirmed that the release mechanism provided a clean step input. The measured oscillation frequency of the vane with this known moment constant provided a check of the calculated moment of inertia of the vane. Tests with a simulated aerodynamic drag load applied at the outboard sleeve bearing indicated that a damping-ratio component of about 0.05 was contributed by friction.

## Flight Experience

The load capabilities of the vane assembly have been demonstrated primarily in flight tests rather than by laboratory testing. The vane has been used successfully in a number of flights, both subsonic and supersonic, where the dynamic pressure has exceeded  $38.3 \text{ kN/m}^2$  (800 psf). Flights at a Mach number of about 2.5 caused some heating discoloration and would appear to define a limiting thermal condition for the vane. In figure 10 are plotted a number of flight conditions at high dynamic pressures where the vanes have been used successfully; also shown is a line of constant dynamic pressure for reference.

Many flight tests in which these vanes were used have involved storm penetrations where rain or hail were encountered. Hail on a few flights damaged the vanes. During subsonic flight, the rain or supercooled water particles did not appear to affect the vanes. At supersonic speeds, however, the ice crystals or water droplets apparently eroded the fiber-glass covering of the leading edge and the metal-wood joint with the subsequent loss of the balsa-wood section of the flow vane.

## CONCLUDING REMARKS

Tests of a low-inertia flow-direction vane have indicated satisfactory performance for the in-flight measurement of gust velocities. There are some nonlinearities apparent in the aerodynamic torque and damping ratio; however, at small angles of attack, the vane can be treated as a single-degree-of-freedom, second-order system in predicting response limitations or in making response corrections.

The test data indicate that at the subsonic conditions of these tests the vane has a natural frequency of  $0.45\sqrt{q}$  (for dynamic pressure  $q$  measured in  $N/m^2$ ) or  $3.1\sqrt{q}$  (for  $q$  measured in psf). For incompressible flow, this corresponds to a frequency of about 0.18 Hz per knot indicated airspeed. At the supersonic condition of these tests, the vane has a natural frequency of  $0.42\sqrt{q}$  (for  $q$  measured in  $N/m^2$ ) or  $2.9\sqrt{q}$  (for  $q$  measured in psf). The measured damping ratio for the vane was 0.80 to 0.65 critical at sea level and it decreased essentially as the square root of the air density.

Force measurements made during subsonic tests indicate that the center-of-pressure location for the vane is at about 11.3 percent chord. This result indicates that for a vane of this general design, care must be taken to make the mass balance ahead of the pivot axis aerodynamically ineffective. Full-span balance weights which extend the leading edge significantly forward of the pivot axis may make the vane almost neutrally stable.

Langley Research Center,  
National Aeronautics and Space Administration,  
Hampton, Virginia, February 13, 1971.

#### REFERENCES

1. Rhyne, Richard H.; and Steiner, Roy: Power Spectral Measurement of Atmospheric Turbulence in Severe Storms and Cumulus Clouds. NASA TN D-2469, 1964.
2. Gersten, Klaus: Nonlinear Airfoil Theory for Rectangular Wings in Incompressible Flow. NASA RE 3-2-59W, 1959.
3. Winter, H.: Flow Phenomena on Plates and Airfoils of Short Span. NACA TM 798, 1936.
4. Michael, William H., Jr.: Flow Studies in the Vicinity of a Modified Flat-Plate Rectangular Wing of Aspect Ratio 0.25. NACA TN 2790, 1952.

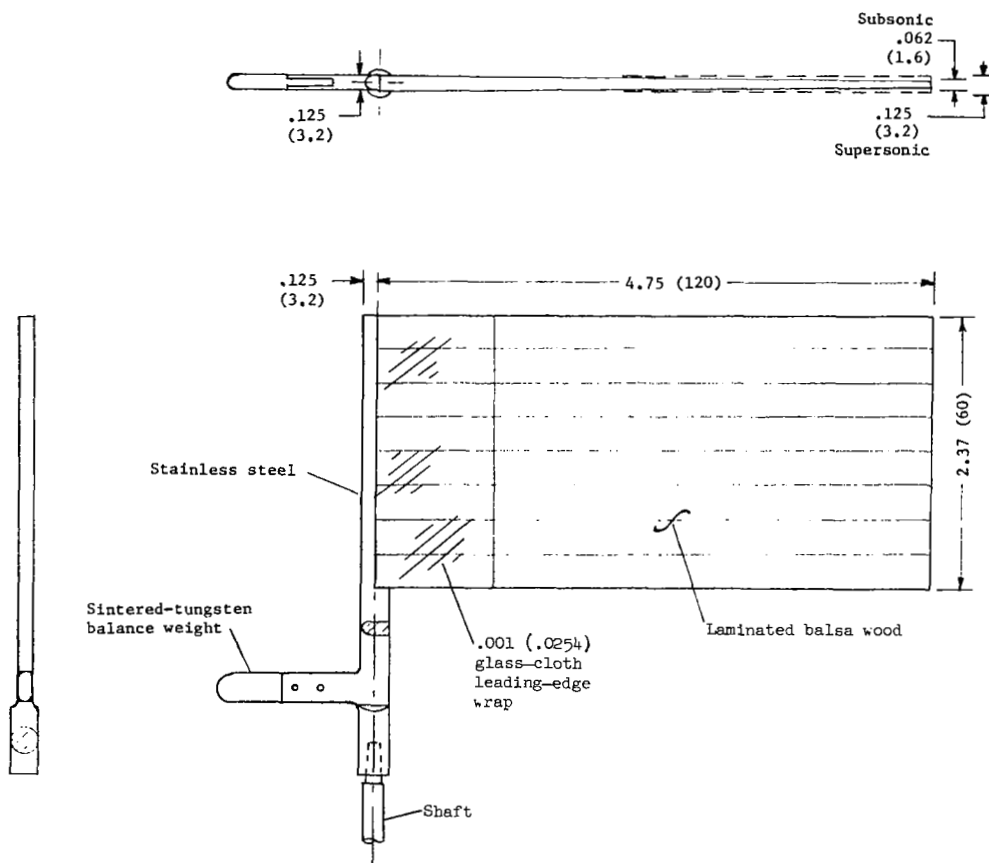
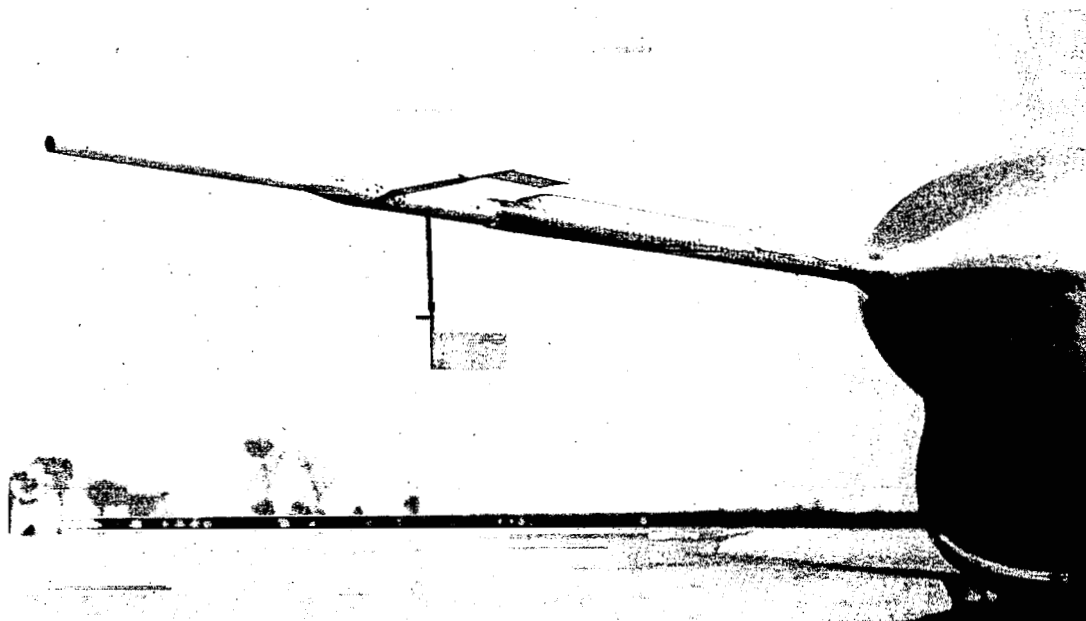
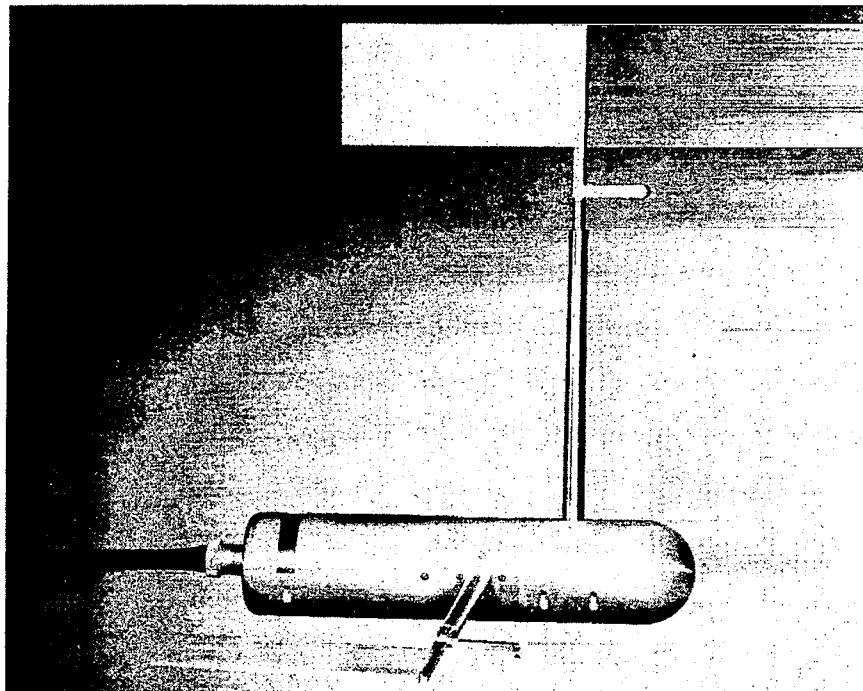


Figure 1.- Flow-direction vane. (Dimensions are in inches (mm).)



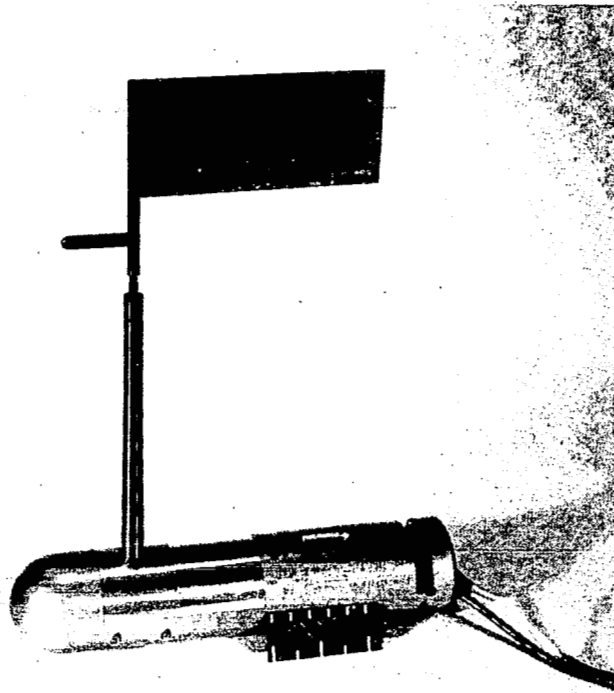
L-59-7612

Figure 2.- Installation of combined pitot-static tube, flow-direction transducer on test airplane.



L-68-1673

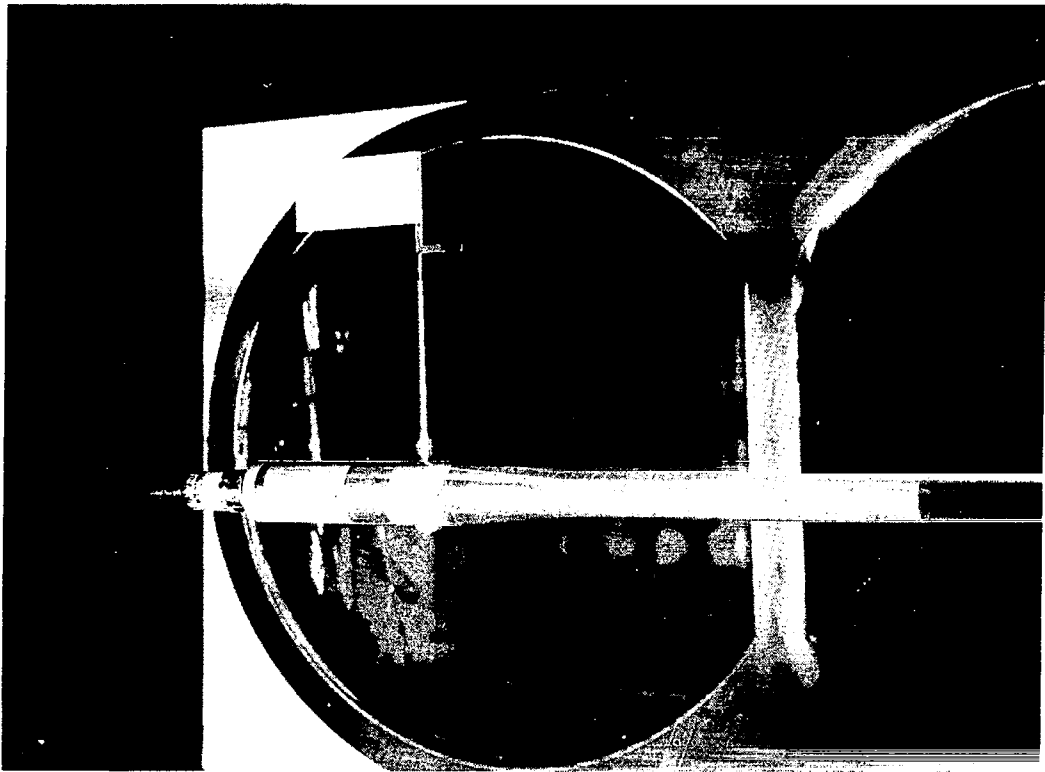
Figure 3.- Flow-direction transducer.



L-69-1480

Figure 4.- External view of vane test unit  
for subsonic tests.





L-69-8564

Figure 5.- Vane test unit modified for supersonic tests and mounted in Langley 4- by 4-foot supersonic pressure tunnel.

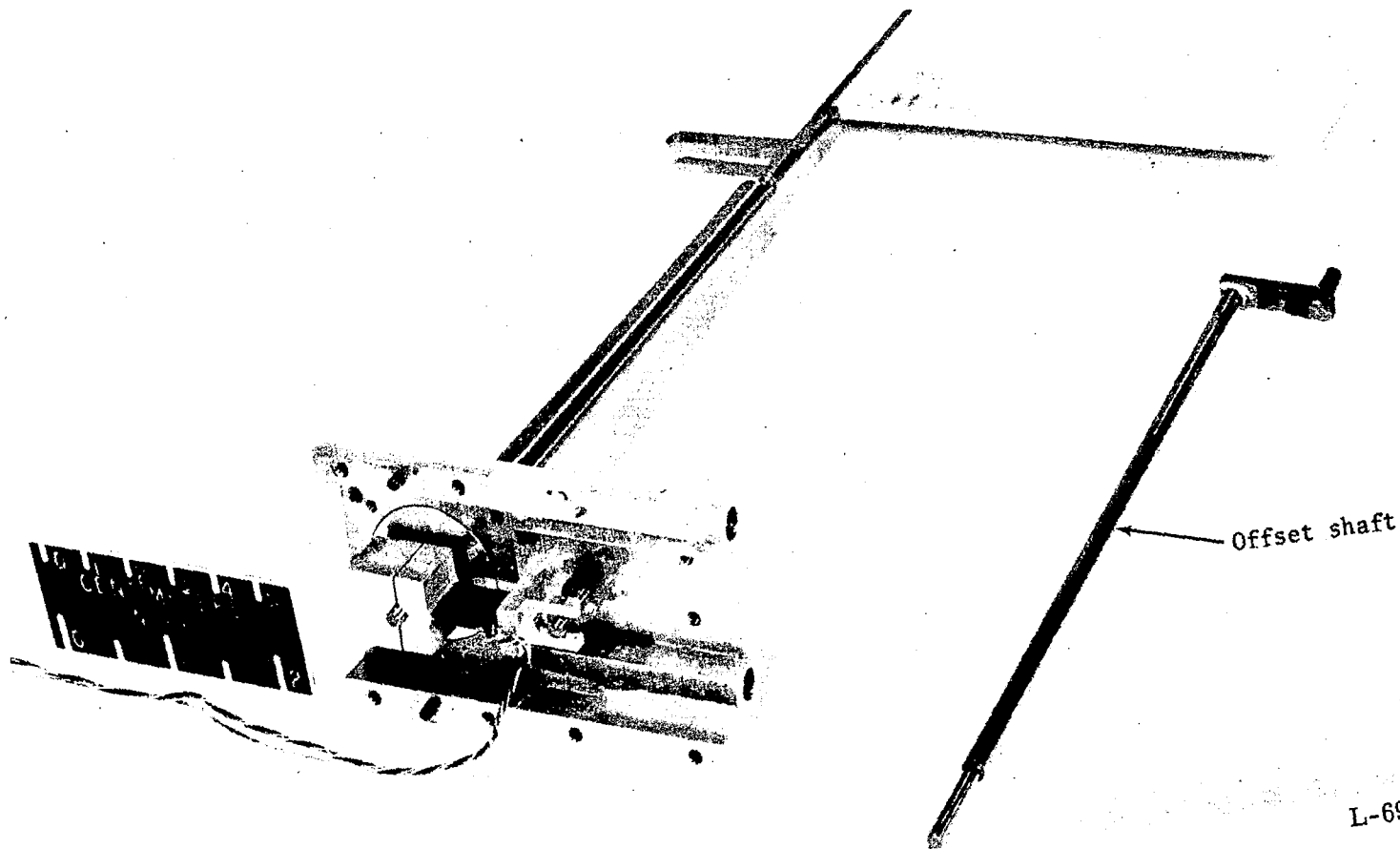
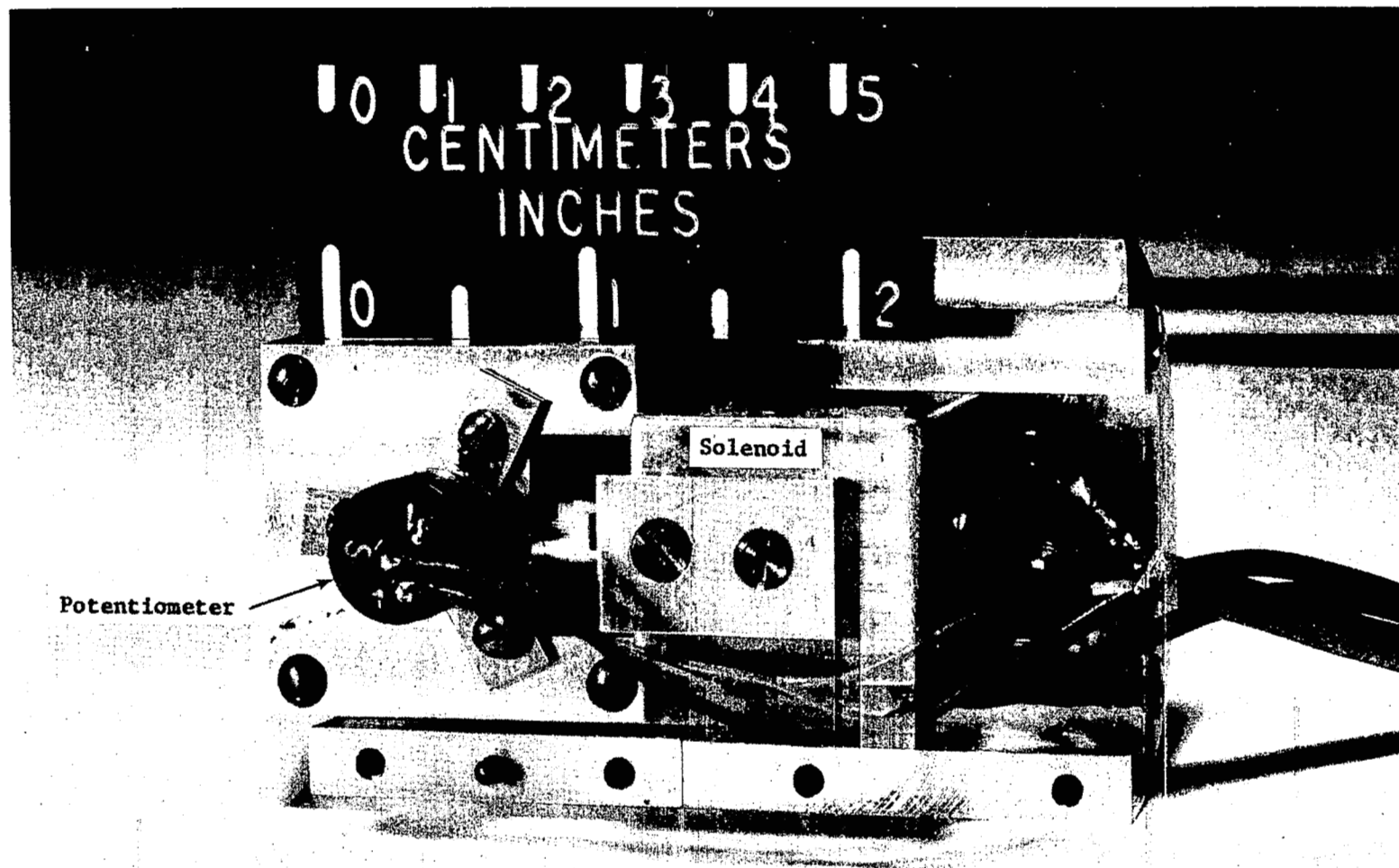


Figure 6.- Details of force-test apparatus.



L-69-1481.1

Figure 7.- View of interior mechanism for dynamic-test apparatus.

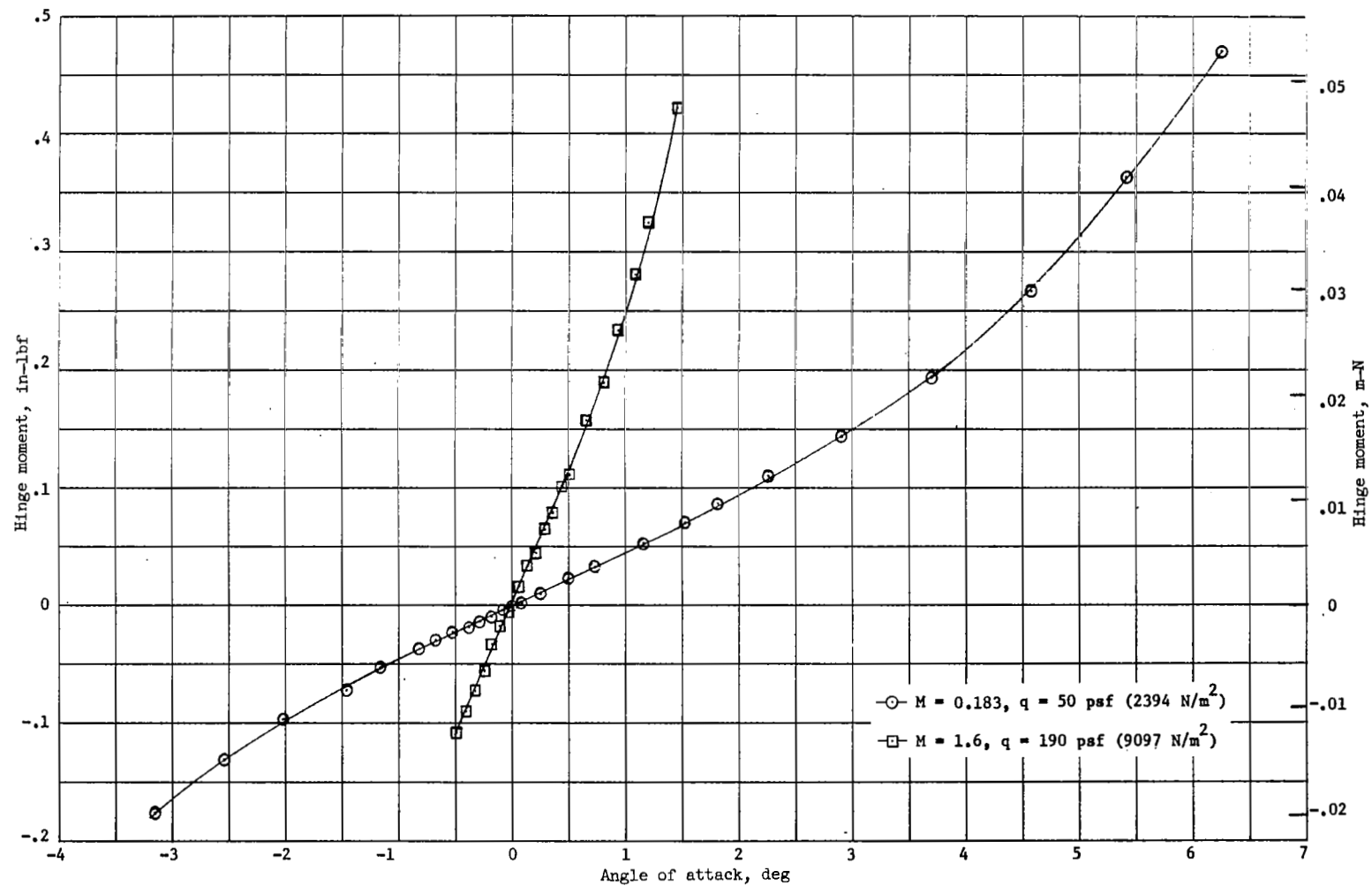
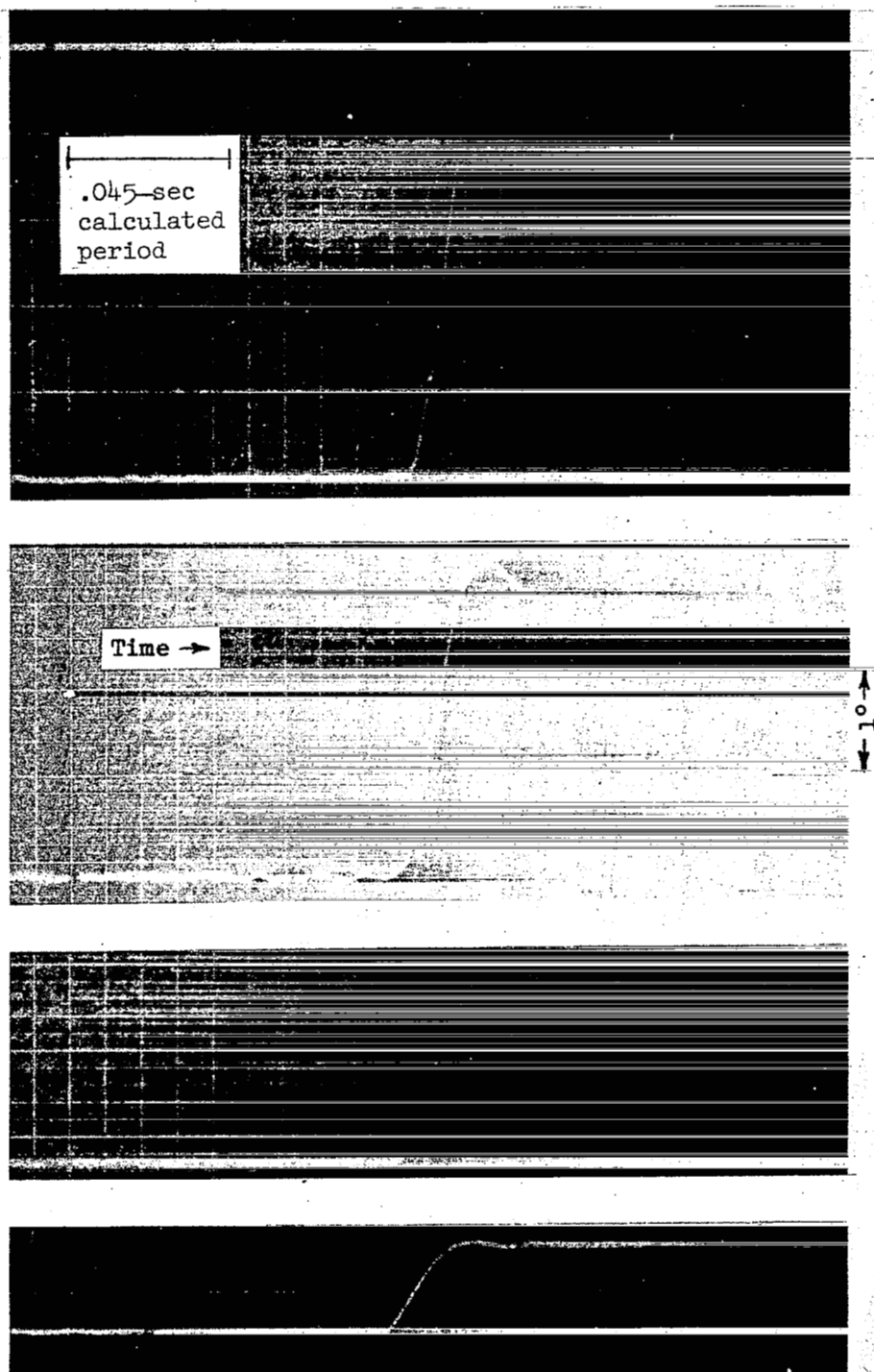


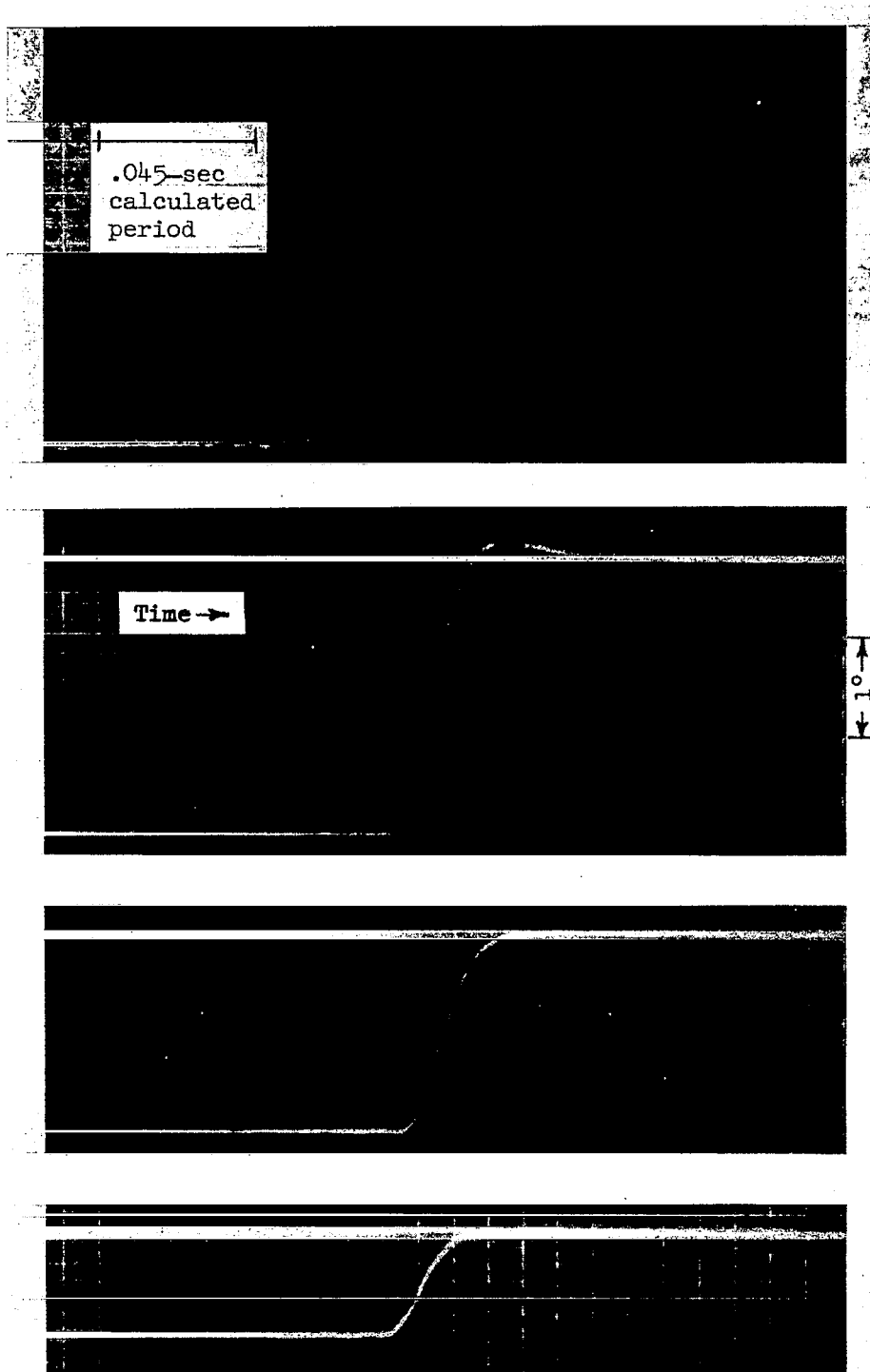
Figure 8.- Plots of vane hinge moments as a function of angle of attack measured under two test conditions.  
Data corrected for vane deflection.



(a) Test condition 1:  $M = 0.183$  and sea-level density.

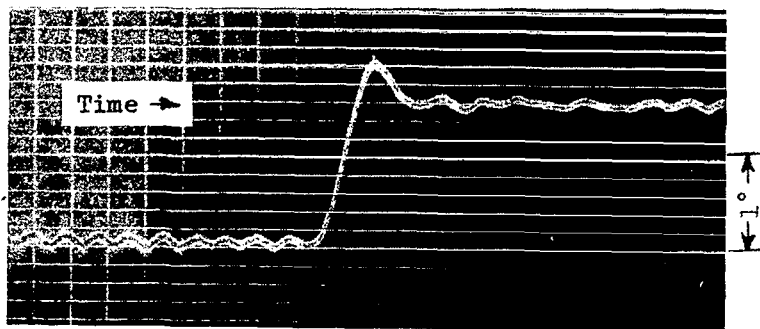
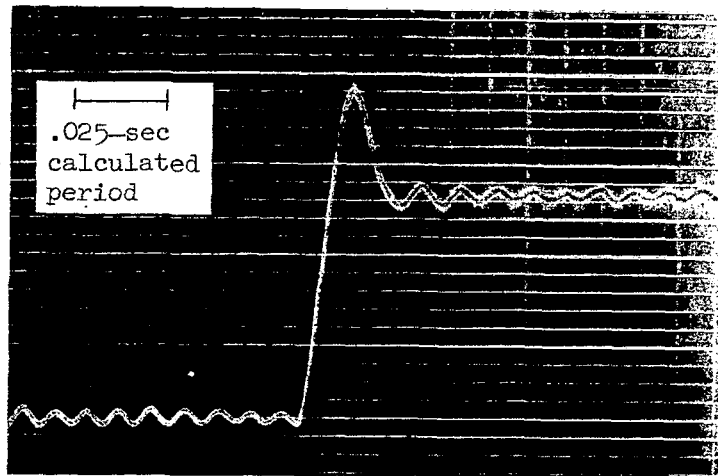
Figure 9.- Reproductions of time histories for vane releases from various initial angles of attack (about  $1^\circ$  to  $4^\circ$ ).

should be  
ed.



(b) Test condition 2:  $M = 0.268$  and 0.47-sea-level density.

Figure 9.- Continued.



(c) Test condition 3:  $M = 1.6$  and 0.073-sea-level density.

Figure 9.- Concluded.

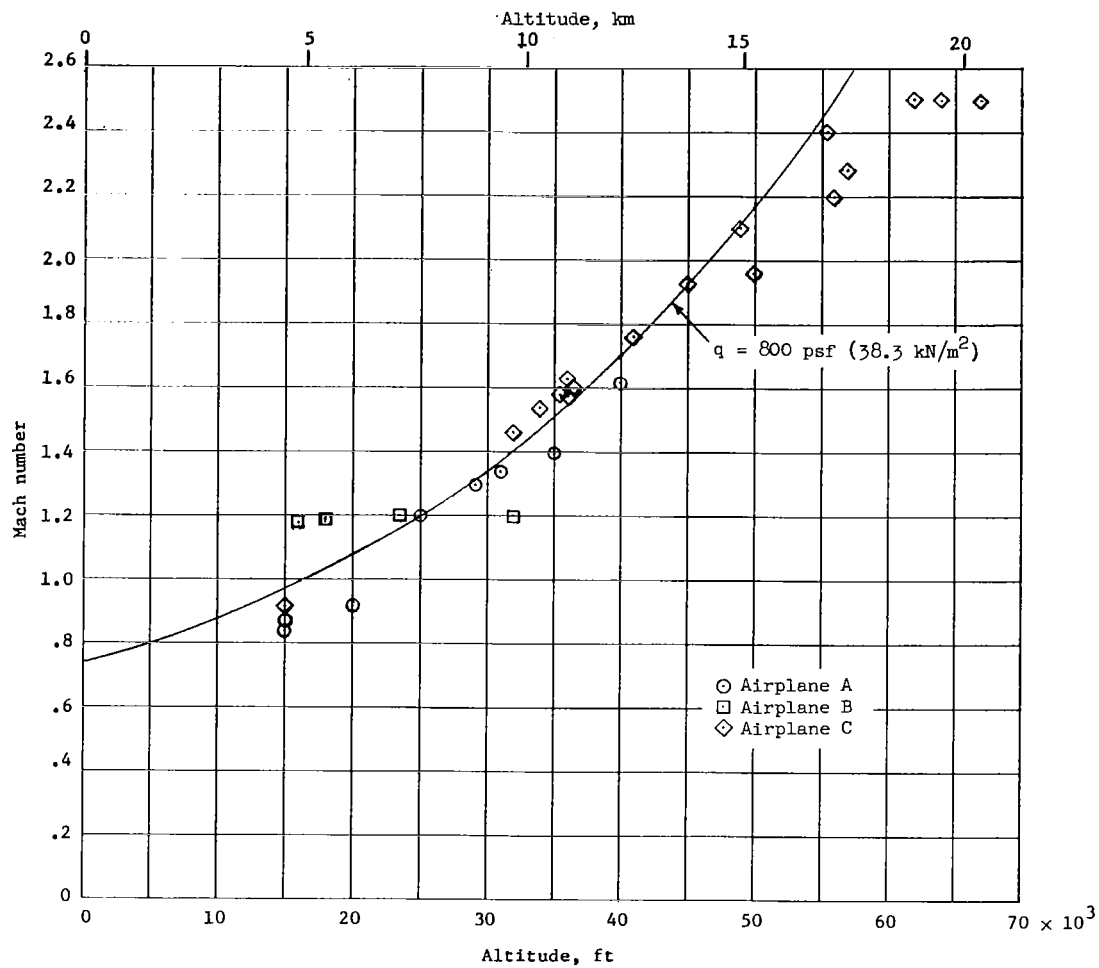


Figure 10.- Plot of some flight conditions where the vanes have been used successfully at high dynamic pressures.